RSC Advances

PAPER

View Article Online
View Journal | View Issue

Cite this: *RSC Adv.*, 2020, **10**, 16209

Stereoselective polymerization of methyl methacrylate and *rac*-lactide mediated by iminomethylpyridine based Cu(II) complexes†

Jaegyeong Lee,[a] Minyoung Yoon,[a] Hyosun Lee *[a] and Saira Nayab*[b]

Iminomethylpyridine based copper(II) complexes $[L_nCuCl_2]$ (L_n = L_A, L_C–L_F) and $[L_BCu(\mu\text{-}Cl)Cl]_2$ have been synthesized and characterized. $[L_CCuCl_2]$ and $[L_ECuCl_2]$ were identified to possess distorted square pyramidal geometries obtained *via* *N*,*N*′-bidentate coordination, whereas $[L_FCuCl_2]$ showed *N*,*N*′,*N*″-coordination of the corresponding ligand (L_F). $[L_BCu(\mu\text{-}Cl)Cl]_2$ was found to be dimeric with a distorted square pyramidal geometry around the Cu(II) center. The catalytic properties of dimethyl derivatives, generated *in situ*, towards the ring opening polymerization (ROP) of *rac*-LA were investigated. All the complexes efficiently polymerized *rac*-LA and yielded heterotactic poly(lactide) (PLA) (P_r up to 0.88 at −25 °C). Further, these complexes could effectively polymerize methyl methacrylate (MMA) at 60 °C in the presence of modified methylaluminoxane (MMAO), to furnish syndio-enriched PMMA. The catalytic efficacies of synthesized complexes can be correlated to the suitable complexity of the substituents attached to the ligand architecture. Thus, both the steric and electronic properties as well as the orientation of the various substituents relative to the *xy* plane of the pyridyl moiety and metal center play an influential role in steering catalytic activities, whereas the selectivities remain unaffected.

Received 27th January 2020
Accepted 16th April 2020

DOI: 10.1039/d0ra00805b

rsc.li/rsc-advances

1. Introduction

Schiff bases and their derivatives have attracted considerable attention owing to their excellent synthetic flexibility, thermal stability, selectivity, and sensitivity towards the central metal atom.[1–4] Schiff bases are considered as privileged ligands due to their excellent chelating abilities to furnish stable coordination complexes with a variety of metals, since they exhibit structural variations from *N*,*N*′-bidentate to *N*,*N*′,*X*-tridentate and *N*,*N*′,*N*,*X*′-tetradentate.[5–7] Metal complexes ligated to Schiff base derivatives are endowed with a wide range of interesting properties appropriate for application in fields such as catalysis,[8,9] medicine,[10,11] crystal engineering[12] as an anti-corrosion agent,[13] photochemistry,[14] biochemistry,[15] organic synthesis,[16] and materials science.[17] More recently, transition metal complexes coordinated to the *N*-substituted *N*,*N*′- or *N*,*N*′,*N*″-iminomethylpyridine derivatives proved to be promising candidates for selective catalysts[18] and were successfully employed as ligands in various applications.[19–21] For instance, Hsiao[22] described the synthesis of Cu(II) complexes with iminopyridine ligands for atom transfer radical polymerization (ATRP). Similarly, iminomethylpyridine-based Fe(II) and Mo(0) complexes for the polymerization of MMA were reported to furnish syndio-enriched PMMA.[23,24]

Stereocontrol is of high importance during polymerization, as tacticity affects key mechanical properties of polymers, such as crystallinity, thermal behaviors and brittleness. Apart from mechanical properties, gas permeation and chemical degradation profile are also dependent on stereochemical makeup of polymer.[25] However, careful choice of ligand architecture is mandatory to create stereo-controlled polymer. For instance, Marks and coworkers[26] showed that chiral *ansa*-bridged lanthanocenes give isotactic or syndiotactic PMMA based on the ligand assembly. Similarly, Yasuda and coworkers[27] reported that Cp_2*LnR (Ln = Sm or Yb) catalyzed highly syndiotactic PMMA. Schiff base derived late transition metal complexes, such as (α-diimine)-based nickel complexes, pyridylbisimine-based Fe(II) and Co(II), iminopyridine- or aminopyridine-based Fe(II) complexes polymerized MMA to give syndio-enriched PMMA.[28] Schiff based derived-Zn(II) complexes displayed excellent catalytic performance with mediocre to high stereoselectivities.[29,30] The design and synthesis of tridentate *N*,*N*′,*N*″-Schiff bases ligands for controlled polymerization of polar monomers have been recently disclosed.[31,32] In this regard, we have recently employed Pd(II), Zn(II), Cu(II) and Cd(II) initiators supported with iminomethylpyridine derived Schiff bases

[a]*Department of Chemistry, Green-Nano Materials Research Center, Kyungpook National University, 80 Daehakro, Bukgu, Daegu, 41566, Republic of Korea. E-mail: hyosunlee@knu.ac.kr; Fax: +82-53-950-6330; Tel: +82-53-950-5337*

[b]*Department of Chemistry, Shaheed Benazir Bhutto University, Sheringal Dir (U), Khyber Pakhtunkhwa, Islamic Republic of Pakistan. E-mail: drnayab@sbbu.edu.pk; sairanayab07@yahoo.com*

† Electronic supplementary information (ESI) available: $[L_BCu(\mu\text{-}Cl)Cl]_2$, $[L_CCuCl_2]$, $[L_ECuCl_2]$, and $[L_FCuCl_2]$. CCDC 1977263–1977266. For ESI and crystallographic data in CIF or other electronic format see DOI: 10.1039/d0ra00805b

towards stereoselective ROP of *rac*-LA and MMA polymerization. These catalysts were effective and afforded high-molecular-weight PLAs and PMMAs with mediocre to high syndiotacticities.[33–38] As an extension of our continuous interest in the stereoselective ROP of *rac*-LA and MMA polymerization, we synthesized Cu(II) complexes ligated to iminomethylpyridine derivatives and investigated their catalytic efficacy in MMA and *rac*-LA polymerization in this study.

2. Experimental

2.1. General considerations

All reactions were performed using standard Schlenk techniques under an atmosphere of high-purity argon or using glovebox techniques. All the starting materials including $CuCl_2 \cdot 2H_2O$, 2-pyridinecarboxaldehyde, *N*,*N*-dimethylethylenediamine, 2-methoxyethylamine, 1-(2-aminoethyl)piperidine, 4-(2-aminoethyl)morpholine, 3-(dimethylamino)-1-propylamine, 3-methoxypropylamine, magnesium sulfate ($MgSO_4$), molecular sieve (0.4 nm), methyl lithium solution (1.6 M in diethyl ether), and methyl methacrylate (MMA) were purchased from Aldrich and Merck. Anhydrous solvents such as acetone, ethanol (EtOH), dimethylformamide (DMF), diethyl ether (Et_2O), and dichloromethane (CH_2Cl_2), *n*-pentane and *n*-hexane were purchased from Merck and used without further purification. Modified methylaluminoxane (MMAO) was purchased from Tosoh Finechem. Corporation as a 5.90 wt% aluminum in toluene solution and used without further purification. 3,6-Dimethyl-1-dioxane-2,5-dione (*rac*-LA) was purchased from Aldrich and stored in a glove box. Toluene and THF were dried by refluxing over sodium and benzophenone, and then distilled under argon and stored over activated molecular sieves (4 Å) for 24 h in a glovebox prior to use. $CDCl_3$, C_6D_6, and $C_2D_2Cl_4$ were dried over activated 4 Å molecular sieves. CH_2Cl_2 and *n*-hexane were dried over CaH_2 for 48 h, distilled under argon, and stored over activated molecular sieves (4 Å) in a glovebox prior to use.

The ligands (*E*)-N^1,N^1-dimethyl-N^2-(pyridin-2-ylmethylene) ethane-1,2-diamine (**L_A**),[39] (*E*)-2-methoxy-*N*-(pyridin-2-ylmethylene)ethanamine (**L_B**),[40] (*E*)-2-(piperidin-1-yl)-*N*-(pyridin-2-ylmethylene)ethanamine (**L_C**),[41] (*E*)-2-morpholino-*N*-(pyridin-2-ylmethylene)ethanamine (**L_D**),[38] (*E*)-N^1,N^1-dimethyl-N^3-(pyridin-2-ylmethylene)propane-1,3-diamine (**L_E**),[36] and (*E*)-3-methoxy-*N*-(pyridin-2-ylmethylene)propan-1-amine (**L_F**)[36] were synthesized by a previously reported method. The synthesis of **[L_ACuCl$_2$]** and **[L_DCuCl$_2$]** was carried out as previously reported.[42,43]

^{1}H NMR (operating at 500 MHz) and ^{13}C NMR (operating at 125 MHz) spectra were recorded by a Bruker Avance Digital NMR spectrometer. Chemical shifts were recorded in ppm units (δ) using $SiMe_4$ as an internal standard. Infrared (IR) spectra were recorded on Bruker FT/IR-Alpha (neat) instrument and data were reported in cm^{-1}. Elemental analyses (C, H, and N) of the prepared complexes were carried out using an elemental analyzer (EA 1108; Carlo-Erba, Milan, Italy). GPC analysis of PLA samples was performed at room temperature using THF as the eluent on a Waters Alliance GPCV2000 instrument equipped with differential refractive index detectors and calibrated using monodisperse polystyrene (PS) standards at a flow rate of 1.0 mL min^{-1}. Number-average molecular weight (M_n) and PDI values of the polymers are given relative to PS standards. Microstructural analysis of obtained PLA was determined by inspecting the methine proton region of the homodecoupled ^{1}H NMR spectra (Fig. S4 and S5†).[44] The probability of heterotactic enchainment (P_r values) was calculated using the equation $P_r = 2I1/(I1 + I2)$ where $I1 = (sis + sii)$ and $I2 = (iis + iii + isi)$.[45,46] Microstructural analysis of PMMA was carried out using ^{1}H NMR and it was classified as syndiotactic (rr, 0.85 ppm), heterotactic (mr, 1.02 ppm), and isotactic (mm, 1.21 ppm).[47,48] The representative ^{1}H NMR spectrum for calculating tacticity of PMMA is shown in Fig. S1.† The glass transition temperature (T_g) was measured using a thermal analyzer (DSC 4000; PerkinElmer).

2.2. Synthesis

2.2.1 2-Methoxy-*N*-(pyridin-2-ylmethylene)ethanamine(dichloro)copper(II), [L_BCu(μ-Cl)Cl]$_2$. A solution of **L_B** (0.821 g, 5.00 mmol) in anhydrous EtOH (10.0 mL) was added to a solution of $CuCl_2 \cdot 2H_2O$ (0.852 g, 5.00 mmol) in anhydrous EtOH (10.0 mL) and stirred at room temperature for 12 h to form a green powder. The solid was filtered and washed with cold EtOH (20.0 mL × 2), followed by washing with Et_2O (20.0 mL × 3). The resultant solid was dried under vacuum to yield **[L_BCu(μ-Cl)Cl]$_2$** as a final product (1.37 g, 92%). Analysis calculated for $C_9H_{12}Cl_2CuN_2O$ (%): C, 36.2; H, 4.05; N, 9.38. Found: C, 36.0; H, 4.02; N, 9.19. FTIR (solid neat; cm^{-1}): ν(C–H) 2915 w; ν(C=C) 1651 m; ν(C=N)/py and ν(C=C)py 1474 m and 1436 m; δ(–C–H sp^3) 1306 m; ν(N–C) 1227 s; ν(C–O) 1112 (s); δ(C–H sp^2) 837 m.

2.2.2 2-(Piperidin-1-yl)-*N*-(pyridin-2-ylmethylene)ethanamine(dichloro)copper(II), [L_CCuCl$_2$]. An analogous method described for **[L_BCu(μ-Cl)Cl]$_2$** was adopted for the synthesis of **[L_CCuCl$_2$]**, except utilizing **L_C** (1.09 g, 5.00 mmol) and $CuCl_2 \cdot 2H_2O$ (0.852 g, 5.00 mmol) to get the final product (1.44 g, 82%). Analysis calculated for $C_{13}H_{19}Cl_2CuN_3$ (%): C, 44.4; H, 5.44; N, 12.0. Found: C, 44.6; H, 5.48; N, 11.9. FTIR (solid neat; cm^{-1}): ν(C–H) 2935 w; ν(C=C) 1656 m; ν(C=N)/py and ν(C=C)py 1599 m and 1462 w; δ(–C–H sp^3) 1326 m; ν(N–C) 1215 s; δ(C–H sp^2) 860 m.

2.2.3 N^1,N^1-Dimethyl-N^3-(pyridin-2-ylmethylene)propane-1,3-diamine(dichloro)copper(II), [L_ECuCl$_2$]. An analogous method described for **[L_BCu(μ-Cl)Cl]$_2$** was adopted for the synthesis of **[L_ECuCl$_2$]**, except utilizing **L_E** (0.956 g, 5.00 mmol) and $CuCl_2 \cdot 2H_2O$ (0.852 g, 5.00 mmol) to yield the final product (1.51 g, 93%). Analysis calculated for $C_{11}H_{17}Cl_2CuN_3$ (%): C, 40.6; H, 5.26; N, 12.9. Found: C, 40.7; H, 5.24; N, 12.9. FTIR (solid neat; cm^{-1}): ν(C–H) 2896 w; ν(C=C) 1636 w; ν(C=N)/py and ν(C=C)py 1590 m and 1438 w; δ(–C–H sp^3) 1385 m; ν(N–C) 1226 s; δ(C–H sp^2) 855 m.

2.2.4 3-Methoxy-*N*-(pyridin-2-ylmethylene)propan-1-amine(dichloro)copper(II), [L_FCuCl$_2$]. An analogous method described for **[L_BCu(μ-Cl)Cl]$_2$** was adopted for the synthesis of **[L_FCuCl$_2$]**, except utilizing **L_F** (0.891 g, 5.00 mmol) and $CuCl_2 \cdot 2H_2O$ (0.852 g, 5.00 mmol) to yield the final product (1.33 g, 85%). Analysis calculated for $C_{10}H_{14}Cl_2CuN_2O$ (%): C, 38.4; H,

4.51; N, 8.96. Found: C, 38.7; H, 4.51; N, 8.98. FTIR (solid neat; cm^{-1}): ν(C–H) 3017 w; ν(C=C) 1647 s; ν(C=N)/py and ν(C=C)py 1597 m and 1476 w; δ(–C–H sp^3) 1449 m; ν(N–C) 1221 s; ν(C–O) 1118 (s); δ(C–H sp^2) 871 m.

2.3. Crystal structure determination

An X-ray-quality single crystal was coated with paratone-N oil and the diffraction data were acquired at different temperatures and wavelengths. At 100(2) K, the X-ray diffraction data of **[L_BCu(μ-Cl)Cl]$_2$** and **[L_ECuCl$_2$]** were collected using synchrotron radiation with $\lambda = 0.63000$ and 0.61000 Å, respectively. At 200(2) K, the X-ray diffraction data of **[L_CCuCl$_2$]** and **[L_FCuCl$_2$]** were collected using home machine X-ray source ($\lambda = 0.71073$ Å) and synchrotron radiation ($\lambda = 0.610$ Å), respectively. The synchrotron X-ray diffraction data were collected using a Rayonix MX225HS CCD area detector at 2D SMC with a silicon (111) double crystal monochromator (DCM) at the Pohang Accelerator Laboratory, South Korea. The PAL BL2D-SMDC Program[49] was used for data collection (detector distance is 66 mm, omega scan; $\Delta\omega = 1^\circ$, exposure time varies 0.1–1 s per frame depending on the size of crystals) and HKL3000sm (Ver. 703r)[50] was used for cell refinement, reduction, and absorption correction. The home machine X-ray diffraction data was collected using Bruker a APEX-II detector and sealed Mo Kα X-ray source ($\lambda = 0.71073$) with graphite monochromator. The Bruker SMART was used for data collection and cell refinement. The data reduction and absorption correction was done using Bruker SAINT and Bruker SADABS program, respectively. Structures were solved by direct methods, and refined by full-matrix least-squares refinement using the SHELXL-2018 (ref. 51) computer program. The positions of all non-hydrogen atoms were refined with anisotropic displacement factors. All hydrogen atoms in **[L_BCu(μ-Cl)Cl]$_2$**, **[L_CCuCl$_2$]**, and **[L_FCuCl$_2$]** were placed using a riding model, and their positions were constrained relative to their parent atoms using the appropriate HFIX command in SHELXL-2018. All hydrogen atoms in **[L_ECuCl$_2$]** were found in difference Fourier map and refined isotopically. X-ray crystallography with PLS-II 2D-SMC beamline was supported by MSIP and POSTECH. The crystallographic refinements and structural data of **[L_BCu(μ-Cl)Cl]$_2$**, **[L_CCuCl$_2$]**, **[L_CCuCl$_2$]**, and **[L_CCuCl$_2$]** are summarized in Table S1.†

2.4. Ring opening polymerization of *rac*-LA

In the polymerization of *rac*-LA using a dimethyl copper initiator, the active catalyst species were generated as follows. Under dry argon conditions, dried THF (7.35 mL) was added to a 100 mL Schlenk flask containing the complex (**[L_ACuCl$_2$]** (0.156 g, 0.50 mmol), **[L_BCu(μ-Cl)Cl]$_2$** (0.149 g, 0.50 mmol), **[L_CCuCl$_2$]** (0.176 g, 0.50 mmol), **[L_DCuCl$_2$]** (0.177 g, 0.50 mmol), **[L_ECuCl$_2$]** (0.163 g, 0.50 mmol), and **[L_FCuCl$_2$]** (0.156 g, 0.50 mmol)), and stirred to dissolve the complex. To this solution, MeLi (1.00 mmol, 0.65 mL of a 1.6 M solution in Et_2O) was added dropwise to produce the dimethyl Cu(II) species. After stirring at room temperature for 2 h, the THF solution of the resulting dimethyl Cu(II) complex was used to catalyze the ROP of *rac*-LA. The general procedure for the polymerization reaction was as follows. A Schlenk flask (100 mL) was charged with *rac*-LA (0.901 g, 6.25 mmol) under argon atmosphere and 5.00 mL of dried CH_2Cl_2 was added. The polymerization was initiated by slow addition of the catalyst solution (1.0 mL, 0.0625 mmol) *via* a syringe under argon at 25 °C and −25 °C. The reaction mixture was stirred for the specified time and the polymerization reactions were quenched by using H_2O (1.0 mL) followed by the addition of *n*-hexane (2.0 mL) and the solvent was evaporated directly to give sticky polymeric material. The resultant polymeric residue was subjected to monomer conversion determination, which was monitored by integrating monomer *versus* polymer methine resonances in ^{1}H NMR spectrum. The precipitates collected from the bulk mixture were again dissolved with CH_2Cl_2, and sequentially precipitated into *n*-hexane. Solvents were decanted and the white solids were dried *in vacuo* followed by drying in a vacuum oven at 40 °C for 12 h. ^{1}H NMR ($CDCl_3$, 500 MHz) for the obtained polymer: δ 5.13–5.20 (m, 1H), 1.51–1.63 (m, 3H).

The addition of water for quenching is assumed to be resulted in Me/OH chain ends,[52,53] and Cu species being slightly soluble in *n*-hexane and CH_2Cl_2 will remain in solution which was decanted. However, the complete removal of Cu traces from polymer is not confirmed yet, and this pending issue will be investigated in future works.

2.5. MMA polymerization

MMA was purified by distillation before use. Under dry argon conditions, dried toluene (10.0 mL) was added to a 250 mL Schlenk flask containing the complex (**[L_ACuCl$_2$]** (4.68 mg, 15.0 μmol), **[L_BCu(μ-Cl)Cl]$_2$** (4.48 mg, 15.0 μmol), **[L_CCuCl$_2$]** (5.28 mg, 15.0 μmol), **[L_DCuCl$_2$]** (5.31 mg, 15.0 μmol), **[L_ECuCl$_2$]** (4.89 mg, 15.0 μmol), and **[L_FCuCl$_2$]** (4.69 mg, 15.0 μmol)) and stirred to dissolve the catalyst. In this flask, MMAO (modified methylaluminoxane, 5.90 wt% in toluene, 3.80 mL, $[MMAO]_0/[M(II)\ catalyst]_0 = 500$) was added. After the mixture had been stirred for 20 min, MMA (5.00 mL, 47.1 mmol, $[MMA]_0/[M(II)\ catalyst]_0 = 3100$) was transferred to the mixture of catalyst and co-catalyst. The reaction flask was immersed in an oil bath at 60 °C and stirred for 2 h with maintained temperature. The resulting product was placed in a mixture of MeOH (500 mL) and HCl (5.00 mL) and stirred to remove the remaining co-catalyst. The polymer was filtered and washed with MeOH (100 mL × 3) to obtain PMMA, and it was vacuum-dried at 60 °C overnight to remove the solvent.

3. Results and discussion

3.1. Synthesis and properties

Iminomethylpyridine ligands are important building blocks and are known to coordinate easily to transition metals[36–41] These complexes have wide range of applications in catalysis due to their versatile coordination behavior and fine tuning of their stereo-electronic properties. In order to study the effects of different ligand substitution patterns on the polymerization behavior, six substituted 2-iminomethylpyridine derivatives have been selected. For instance, the linker unit variation in **L_A**

and $\mathbf{L_E}$ with an identical iminomethylpyridine framework has been selected to investigate the influence of linking alkyl chain of amine and imine moieties on catalytic activities. For comparison ligands, $\mathbf{L_B}$ and $\mathbf{L_F}$, with an ether arm on imine functionality has been selected, an alkyl chain with an oxygen at fourth or fifth position, respectively, to generate mixed ligand architecture with better δ-donor and π-acceptor properties. To further extend the substituent influence on activity and stereoselectivity, the morpholine and piperidine moieties as closering substituents in $\mathbf{L_C}$ and $\mathbf{L_D}$ have been employed to generate more rigid ligand framework. These iminomethylpyridine ligands (L_n = $\mathbf{L_A}$–$\mathbf{L_F}$) used in the current study were synthesized as reported previously (Fig. 1).[36–41]

A series of new Cu(II) complexes were furnished (in yield = 81–93%) by treating these ligands (L_n = $\mathbf{L_A}$–$\mathbf{L_F}$) with $CuCl_2 \cdot 2H_2O$ in a 1 : 1 molar ratio in EtOH. The resultant Cu(II) complexes were stable in the air and were not affected by the atmospheric constituents and could be stored for months at room temperature. The FTIR spectra of the ligands and their corresponding Cu(II) complexes were compared. The characteristic IR bands assigned to sp^3 ν(C–H), ν(C=N), aromatic ν(C=C), and aromatic ν(C–H) stretch can be observed at ~3000 cm^{-1}, ~1650 cm^{-1}, 1500 cm^{-1} and ~800 cm^{-1}, respectively. In addition, C–O stretch can be identified at 1100 cm^{-1} in ligands containing an oxygen atom. The bands assigned to ν(C=N) of the azomethine group and ν(C=N)py shifted to higher wavenumber in the spectra of all complexes, indicating the possibility of back donation and the participation of nitrogen atoms in bonding.[54,55] Elemental analysis for all complexes was consistent with the proposed structures in Scheme 1. All the synthesized Cu(II) complexes were soluble in common organic solvents.

3.2. Molecular structures of Cu(II) complexes

Single crystals of $[\mathbf{L_BCu(\mu\text{-}Cl)Cl}]_2$ and $[\mathbf{L_ECuCl_2}]$ were obtained using a MeOH/Et_2O system, $[\mathbf{L_CCuCl_2}]$ was obtained by a DMF/Et_2O layer, and $[\mathbf{L_FCuCl_2}]$ was obtained through the acetone/n-pentane solvent diffusion method. The ORTEP diagrams of the complexes; $[\mathbf{L_BCu(\mu\text{-}Cl)Cl}]_2$, $[\mathbf{L_CCuCl_2}]$, $[\mathbf{L_ECuCl_2}]$, and $[\mathbf{L_FCuCl_2}]$ are shown in Fig. 1(a–d) and the detailed bond lengths and angles of complexes are shown in Table S2.† The X-ray structures of $[\mathbf{L_ACuCl_2}]$ and $[\mathbf{L_DCuCl_2}]$ have been published previously.[42,43] $[\mathbf{L_BCu(\mu\text{-}Cl)Cl}]_2$, $[\mathbf{L_CCuCl_2}]$ and $[\mathbf{L_FCuCl_2}]$ were crystallized in a monoclinic crystal system with $P2_1/c$, $P2_1/n$, $P2_1/c$ space groups, respectively, and $[\mathbf{L_ECuCl_2}]$ crystallized in triclinic crystal system with a $P\bar{1}$ space group (Fig. 2).

The $Cu–N_{pyridine}$ and $Cu–N_{imine}$ bond lengths lie in the ranges of 2.032(2)–2.0652(1) Å and 1.967(5)–2.0449(1) Å, respectively, while the average Cu–Cl bond length are observed to be 2.3290 Å. These geometric parameters are within the acceptable range reported for Cu(II) complexes.[56] The characteristic N=C bond lengths of imine moiety are 1.278(3) Å ($[\mathbf{L_BCu(\mu\text{-}Cl)Cl}]_2$), 1.269(7) Å ($[\mathbf{L_CCuCl_2}]$), 1.2751(2) Å ($[\mathbf{L_ECuCl_2}]$), and 1.2703(2) Å ($[\mathbf{L_FCuCl_2}]$), and agreed well with the acceptable value.[57] However, the Cu(1)–O(1) lengths of 4.380 Å ($[\mathbf{L_BCu(\mu\text{-}Cl)Cl}]_2$) and 5.949 Å ($[\mathbf{L_FCuCl_2}]$) were too long to be considered for a coordinative bond. $[\mathbf{L_BCu(\mu\text{-}Cl)Cl}]_2$ has a dimeric structure with a chloro bridge as described previously.[58]

The N(2)–Cu(1)–N(1) and N(3)–Cu(1)–N(2) bond angles in $[\mathbf{L_BCu(\mu\text{-}Cl)Cl}]_2$, $[\mathbf{L_CCuCl_2}]$, $[\mathbf{L_ECuCl_2}]$ and $[\mathbf{L_FCuCl_2}]$ ranged

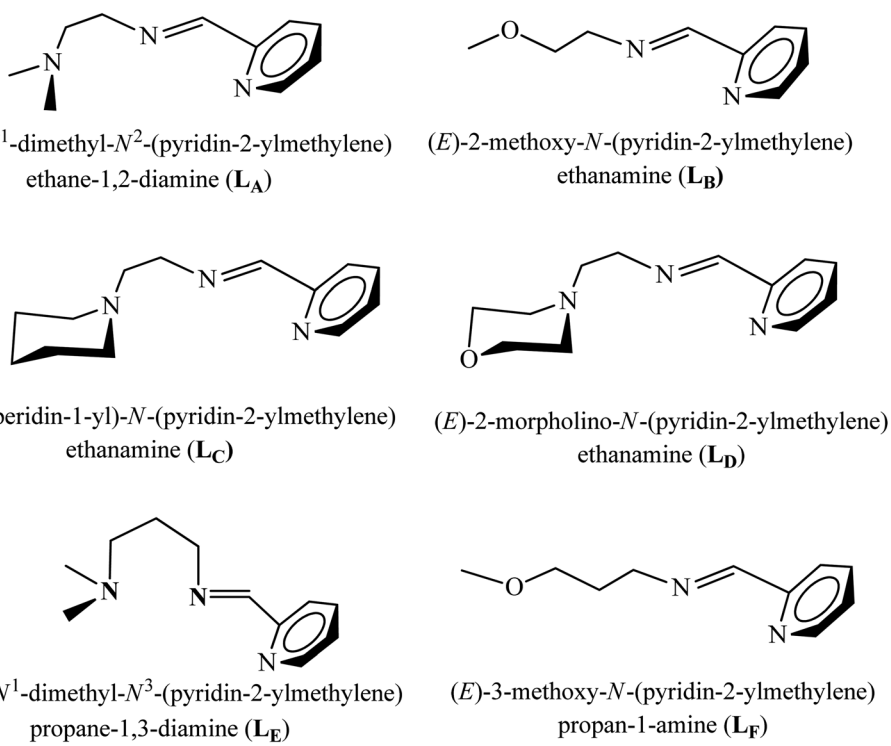

Fig. 1 List of iminomethylpyridine ligands (L_n = L_A–L_F) employed in the complexation to Cu(II) centre.

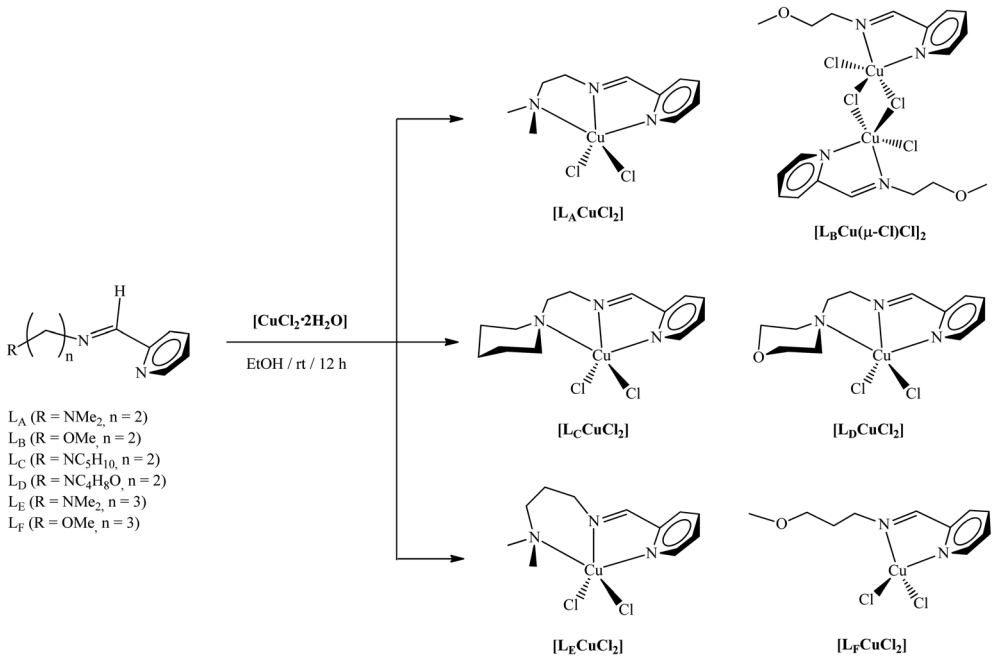

Scheme 1 Synthesis of Cu(II) complexes supported by iminomethylpyridine ligands.

from 78.89(2)° to 82.08(2)° and were affected by the substitution of the five-membered chelate ring.[57] The bond angle of N(3)–Cu(1)–N(2) in **[L_ECuCl_2]** that constituted the six-membered chelate ring were 92.36(5)°, which is similar to the published **[L_ECuBr_2]** angle of 92.24(10)°.[59] The planes of both the piperidine group and the Cu(II) coordination were nearly vertical, and the piperidine group has a stable chair structure.

The structural parameters of the five-coordinated complexes can be obtained using the two largest coupling angles. This τ_5 value is proposed as a simple metric for evaluating

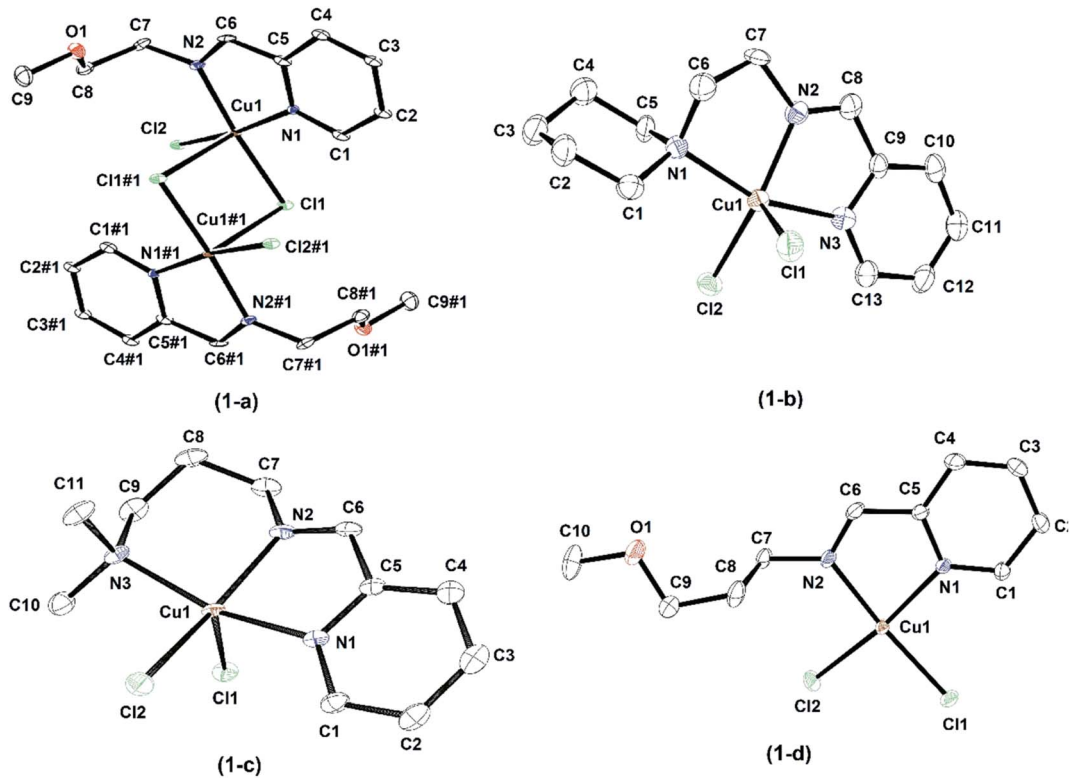

Fig. 2 An ORTEP drawings of [$L_BCu(\mu\text{-}Cl)Cl]_2$ (1-a), [L_CCuCl_2] (1-b), [L_ECuCl_2] (1-c), and [L_FCuCl_2] (1-d) with thermal ellipsoids at 50% probability. All hydrogen atoms have been omitted for clarity.

Table 1 Five-coordinate geometry indices for Cu(II) complexes and representative examples from the literature

Complexes	Geometry	τ_5	Reference
Trigonal bipyramidal (D_{3h})	Trigonal bipyramidal	1.00	58–60
$[L_ACuCl_2]$	Square pyramidal	0.303	42
$[L_BCu(\mu\text{-}Cl)Cl]_2$	Square pyramidal	0.0385	This work
$[L_CCuCl_2]$	Square pyramidal	0.0480	This work
$[L_DCuCl_2]$	Square pyramidal	0.0283	43
$[L_ECuCl_2]$	Square pyramidal	0.0653	This work
$[L_FCuCl_2]$	Square pyramidal	0.0398	This work
Square pyramidal (C_{4v})	Square pyramidal	0.00	58–60

quantitatively the geometry of five-coordinated complexes.[60–62] A comparison of the τ_5 values of Cu(II) complexes is shown in Table 1. The coordination geometry around the metal center of the Cu(II) complexes is depicted as a distorted square pyramid geometry. In the case of dimeric $[L_BCu(\mu\text{-}Cl)Cl]_2$, the two molecules each share one Cl atom, so the dimeric molecule has two bridged Cl groups. Thus, it has a slightly distorted square pyramidal geometry consisting of the two nitrogen atoms and three Cl atoms of the ligand.

3.3. *rac*-LA polymerization

Biodegradable polymers that can display properties that rival poly-olefins are seen as future high-demand materials for a wide range of applications. Efforts have been directed toward decoupling polymeric materials from fossil fuel feedstocks using biological sources[63,64] to decrease the amount of plastic waste ending up in the environment. Our research focuses on the stereoselective ROP of *rac*-LA,[65,66] the efficacy of iminomethylpyridine based Cu(II) complexes to mediate polymerization of *rac*-LA and to focus on the role played by the auxiliary ligand on influencing catalytic efficiency, molecular weight, as well as stereoselectivity. The dimethyl derivatives $[L_nCuMe_2]$ (L_n = L_A–L_F), generated *in situ*, were assessed towards *rac*-LA polymerization at two different temperatures, *i.e.*, 25 and −25 °C. Representative polymerization results are summarized in Tables 2 and 3. All the complexes were able to effectively initiate polymerization at room temperature and afforded PLA with desirable molecular weights and slightly higher PDIs; the heterotacticities were somewhat inferior (P_r values ranged from 0.52 to 0.68; Table 2). Completion of the reaction was confirmed by the absence of the monomer signal in the ^{1}H NMR spectrum. The experimental M_n values (corrected using Mark–Houwink[67,68] factor 0.58) were consistent with the theoretical values, suggesting polymerization at the single reaction site provided by these dimethyl Cu(II) complexes. Slightly higher PDIs of PLAs produced with $[L_nCuMe_2]$ (L_n = L_A–L_F) might be the consequence of backbiting or transesterification side reactions, which results in the formation of macrocycles with a broad molecular weight distribution (PDIs).

It can be suggested that the ROP of *rac*-LA by these initiators is mediated *via* a coordination insertion mechanism.[69,70] In this mechanism, the pre-coordination of the LA molecule to the metal center is crucial for the subsequent ring-opening step.

Table 2 Polymerization of *rac*-LA with dimethyl Cu(II) complexes, $[L_nCuMe_2]$ (L_n = L_A–L_F), generated *in situ* in CH_2Cl_2 at 25 °C

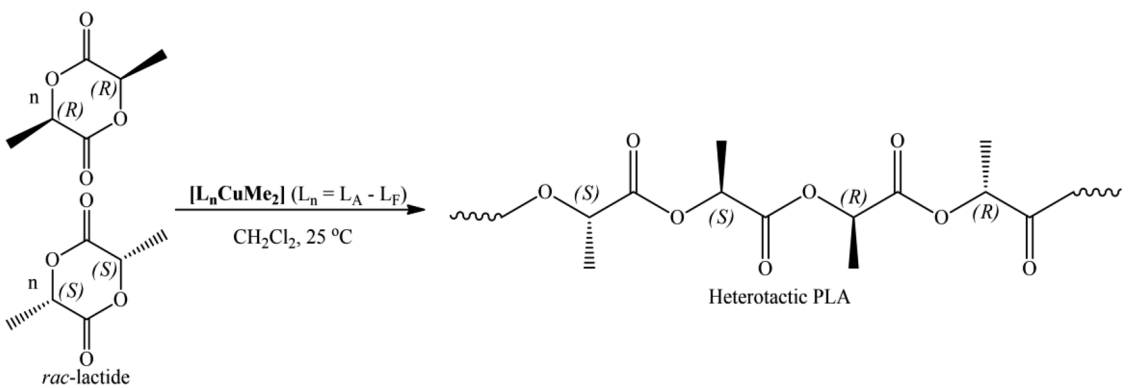

Entry	Catalyst[a]	Conv.[b] (%)	M_n[c] (g mol^{-1}) × 10^3 (calcd)	M_n[d] (g mol^{-1}) × 10^3 (GPC)	PDI[d]	P_r[e]
1	MeLi	99	14.27	11.44	1.50	0.47
2	$[L_ACuMe_2]$	100	14.41	10.92	1.60	0.59
3	$[L_BCu(\mu\text{-}Me)Me]_2$	100	14.41	12.01	1.68	0.52
4	$[L_CCuMe_2]$	100	14.41	12.77	1.52	0.53
5	$[L_DCuMe_2]$	100	14.41	11.49	1.66	0.59
6	$[L_ECuMe_2]$	100	14.41	15.50	1.53	0.59
7	$[L_FCuMe_2]$	100	14.41	9.40	1.81	0.68

[a] Conditions: [initiator] = 0.0625 mmol; [*rac*-LA]/[initiator] = 100; 5.00 mL of CH_2Cl_2 as polymerization solvent; polymerization time = 2 h. [b] Monomer conversion (%) determined by ^{1}H, NMR spectroscopy. [c] Calculated from [molecular weight of *rac*-LA] × [*rac*-LA]/[initiator] × conversion%. [d] Determined by gel permeation chromatography (GPC) in THF, relative to polystyrene standard (corrected using the Mark–Houwink factor of 0.58).[65,66] [e] Probability of heterotactic enchainment (P_r) were calculated on the basis of homonuclear decoupled ^{1}H NMR spectra according to literature.[45,46]

Table 3 Polymerization of *rac*-lactide with *in situ* generated $[L_nCuMe_2]$ ($L_n = L_A$–L_F) from the reaction of $[L_nCuCl_2]$ ($L_n = L_A$–L_F) and MeLi in CH_2Cl_2 at −25 °C

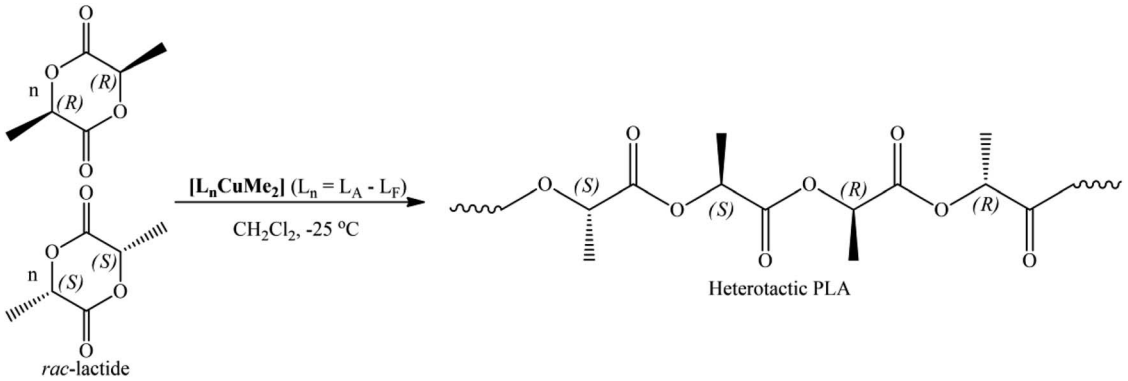

Entry	Catalyst[a]	Conv.[b] (%)	M_n[c] (g mol^{-1}) × 10^3 (calcd)	M_n[d] (g mol^{-1}) × 10^3 (GPC)	PDI[d]	P_r[e]
1	MeLi	99	14.27	11.68	1.46	0.78
2	$[L_ACuMe_2]$	100	14.41	33.61	1.53	0.84
3	$[L_BCu(\mu\text{-}Cl)Me]_2$	99	14.27	23.57	1.54	0.88
4	$[L_CCuMe_2]$	100	14.41	17.44	1.50	0.83
5	$[L_DCuMe_2]$	97	13.98	10.40	1.25	0.74
6	$[L_ECuMe_2]$	100	14.41	30.01	1.54	0.86
7	$[L_FCuMe_2]$	100	14.41	24.87	1.53	0.87

[a] Conditions: [initiator] = 0.0625 mmol; [*rac*-LA]/[initiator] = 100; 5.00 mL of CH_2Cl_2 as polymerization solvent; polymerization time = 2 h; temp. = −25 °C. [b] Monomer conversion (%) determined by ^{1}H NMR spectroscopy. [c] Calculated from [molecular weight of *rac*-LA] × [*rac*-LA]/[initiator] × conversion%. [d] Determined by gel permeation chromatography (GPC) in THF, relative to polystyrene standard (corrected using the Mark–Houwink factor of 0.58).[65,66] [e] Probability of heterotactic enchainment (P_r) were calculated on the basis of homonuclear decoupled ^{1}H NMR spectra according to literature.[45,46]

The alkyl group then acts as a nucleophile and opens the LA ring (Scheme S1†). Blank polymerizations (entry 1 in Table 2) were also performed in the presence of MeLi alone, where PLA was obtained slowly with negligible stereoselectivity. These results suggest a role of the Lewis metal center and the ligand architecture that offers better polymerization control and steers the stereoselectivity of the resultant polymer.

The microstructural analysis revealed dimethyl Cu(II) complexes in the current study yielded hetero-enriched PLAs. It is evident from the polymerization data that preference for heterotactic enchainment is lower at room temperature (Table 2). On the other hand, the complexes $[L_nCuMe_2]$ ($L_n = L_A$–L_F), were able to exhibit better heterotacticities and molecular weight control at −25 °C. For instance, an increase in the P_r values up to 0.88 and slight decrease in PDIs are observed at lower temperatures (Table 3). A closer look at polymerization data revealed no regular tendency of heterotacticity; the stereoselectivity of PLA was not significantly affected by the structure of the ancillary ligands attached to the central metal atom during the polymerization process. These results showed that the heterotacticity is comparable with that of previously reported Cu(II) complexes, but monomer conversion is excellent at lower temperatures. Enhanced heterotacticity was found with these dimethyl Cu(II) initiators bearing the proper complexity of the substituents at the nitrogens of the imine moiety. Heterotactic PLA obtained with these dimethyl Cu(II) complexes proceed *via* chain end-control mechanism, as previously demonstrated by the Darensbourg group for Zn(II) complexes with Schiff bases.[71] Currently, research is underway in our laboratory to fully explain the role of the ROP mechanism and catalyst system, and further research will be concentrated on this.

3.4. MMA polymerization studies

The catalytic competencies of the synthesized Cu(II) complexes were investigated for MMA polymerization in the presence of modified MMAO at 60 °C. The representative polymerization data is tabulated in Table 4. All the complexes effectively polymerized MMA and the resultant polymer was isolated as a white solid and was characterized by GPC in THF using polystyrene standards. All complexes yielded PMMA with a T_g in the range 123–128 °C.

Appropriate ligand architecture plays a pivotal role in endowing a high degree of polymerization control. Generally, the presence of bulky substituents around the metal center negatively affects MMA activation, suggesting that steric bulk of substituents or rigidity of ligand backbone hampered the approach of the monomer to the metal center. For instance, $[L_ECuCl_2]$ displayed a higher activity with a more flexible propylene backbone compared to $[L_ACuCl_2]$ with the ethylene backbone, despite of having identical dimethyl amine substituents (Table 4, entries 3 and 7). However, $[L_CCuCl_2]$ (1.80 ×

Table 4 MMA polymerization by $[L_nCuCl_2]$ ($L_n = L_A$–L_F) complexes in the presence of MMAO

Entry	Catalyst[a]	Yield[b] (%)	Activity[c] (g mol^{-1} cat.·h^{-1}) × 10^4	T_g[d] (°C)	Tacticity % mm	% mr	% rr	M_w[e] (g mol^{-1}) × 10^5	M_w/M_n[f]
1	$CuCl_2 \cdot 2H_2O$[g]	10.8	1.68	129	7.20	23.9	67.5	2.73	1.49
2	MMAO[h]	6.83	1.07	120	37.2	10.9	51.9	1.75	1.37
3	$[L_ACuCl_2]$	10.9	1.71	128	8.54	25.4	66.0	9.76	2.49
4	$[L_BCu(\mu\text{-}Cl)Cl]_2$	11.3	1.77	128	7.97	25.7	66.3	9.79	2.48
5	$[L_CCuCl_2]$	11.5	1.80	128	8.26	25.6	66.1	9.76	2.45
6	$[L_DCuCl_2]$	12.5	1.95	126	7.64	25.6	66.8	9.76	2.49
7	$[L_ECuCl_2]$	12.8	1.98	126	7.78	25.0	67.2	9.96	2.45
8	$[L_FCuCl_2]$	10.7	1.67	123	8.11	25.6	66.2	9.66	2.46

[a] [Cu(II) catalyst]$_0$ = 15 μmol, [MMA]$_0$/[MMAO]$_0$/[Cu(II) catalyst]$_0$ = 3100 : 500 : 1, polymerization temp. = 60 °C and time = 2 h. [b] Yield is defined as (a mass of dried polymer recovered)/(a mass of monomer used). [c] Activity is g of PMMA per mol Cu·h. [d] T_g is glass transition temperature which is determined by a thermal analyzer. [e] Determined by gel permeation chromatography (GPC) eluted with THF at room temperature by filtration with polystyrene calibration. [f] M_n refers to the number average molecular weights of PMMA. [g] It is a blank polymerization in which $CuCl_2 \cdot 2H_2O$ was also activated by MMAO. [h] It is a blank polymerization which was done solely by MMAO.

10^4 g PMMA per mol Cu h) and $[L_DCuCl_2]$ (1.95 × 10^4 g PMMA per mol Cu h), with relatively bulkier piperidine and morpholine substituents and ethylene backbone, displayed higher activities compared to $[L_ACuCl_2]$ (1.77 × 10^4 g PMMA per mol Cu h) in contrast to our previous reports where steric bulk decrease activities.[33] If rigidity or steric hindrance provided by the amine substituents were the only factor that steered the catalytic activity, then one would have expected increased activity with $[L_ACuCl_2]$ bearing dimethyl substituents at the amine moiety, as it provides a more open sphere than $[L_CCuCl_2]$ and $[L_DCuCl_2]$ do, with close ring substituents, but it actually exhibits a lower activity. Thus, it is obvious that appropriate complexity of substituents at the amine nitrogen is crucial for improved activities.

Further, the orientation of the amine substituents relative to the *xy* plane of the pyridine ring and the metal center also influence the activity towards MMA polymerization. $[L_CCuCl_2]$ with the piperidine moiety and $[L_DCuCl_2]$ with the morpholine moiety that are perpendicular and slightly twisted toward the *xy* plane of the *N*-((pyridin-2-yl)methylene)amine-Cu moiety by 64.01° and 69.23° showed slightly lower steric hindrance and exhibited higher activities than $[L_ACuCl_2]$ and $[L_BCu(\mu\text{-}Cl)Cl]_2$ which has distortion angles of 73.83° and 77.61°. In the case of $[L_FCuCl_2]$, the distortion angle was 49.05° and it exhibited lower activities than other copper complexes. In addition, since the Cl atom of adjacent molecules to the planar position, which is perpendicular and slightly twisted (84.76°, 81.86°) plane against the metal plane, are located at a close distance of about 3.0 Å, it could have interfered with the access of the monomer.

Among the synthesized Cu(II) complexes, the L_E-bearing Cu(II) complex exhibited the highest catalytic activity (1.98 × 10^4 g PMMA per mol Cu h) and resulted in PMMA with high molecular weight (9.96 × 10^5 g mol^{-1}) compared to that of the rest of complexes under identical experimental conditions. In addition, it is worth noting that the solubility of complexes in polymerization media showed an impact on the polymerization activity in previous research. Thus, the lower activity of $[L_BCu(\mu\text{-}Cl)Cl]_2$ and $[L_FCuCl_2]$ can also be attributed to its lower solubility in reaction media.

In comparison with our previously reported Cu(II) initiator bearing *N*-methyl-*N*-((pyridin-2-yl)methyl)benzeneamine, the current system was inferior in terms of activities and stereoselectivities but furnished PMMA with high T_g and comparable molecular weights.[72] 2-Iminomethylpyridine- and 2-iminomethylquinoline-based Zn(II) and Pd(II) complexes accomplished syndio-enriched PMMA polymerization with slightly higher activities, which can be attributed to better electrophilicities of Zn(II) and Pd(II) complexes.[31,33] Recently studied *N*,*N*-di(2-picolyl)cyclohexylamine[73] based Pd, Cu, Zn, and Cd complexes for MMA polymerization exhibited lower activities with slightly better syndiotacticities compared to our currently studied catalysts. Similarly, *N*-(2-furanylmethyl)-*N*-(1–3,5-dimethyl-1*H*-pyrazolylmethyl)-*N*-(phenylmethyl)amines-Cu(II) system[74] yielded syndiotactic PMMA (rr = 0.78) with only 30% conversion, whereas Cu(II) complex of 2-(pyrazol-3-yl)-6-(pyrazolate)pyridine and related ligand[75] polymerized MMA with moderate activity and syndiotacticity. Thus, the current catalytic systems proved to be effective in polymerizing MMA and furnished syndio-enriched PMMA with good polymerization control.

To further explore the effect of the ligand and Lewis metal center in the polymerization process, the MMA polymerization was conducted with MMAO alone. A negligible amount of low-molecular-weight PMMA was obtained with almost no stereoregularity. Similarly, no polymer was produced with the dichloro copper(II) complex in the absence of MMAO. The obtained PMMA was syndiotactic with all complexes regardless of the substituents attached to the ligand architecture and coordination mode, whereas the syndiotacticity was higher than that of PMMA made only with the co-catalyst, MMAO. In this study, the syndiotacticity and PDI were not significantly affected by the substituents of ligands around the metal center (Table 4). The activities of the catalyst for MMA and *rac*-LA polymerization can thus be considered to be influenced by the steric and

electronic effect of ligand around the metal. The stereospecific and electronic properties of the substituents did not follow a regular trend for the activity and stereoselectivity.

4. Conclusions

In this work, a new series of Cu(II) complexes supported by 2-iminomethylpyridine ligands were synthesized and characterized by a variety of techniques such as FTIR, elemental analysis, and X-ray diffraction. Distorted square pyramidal geometries were adopted by all the complexes *via* coordinating to ligands in the bi- or tridentate coordination modes. On activation with MMAO, all the complexes displayed moderate activities compared to that of the starting material. **[L_ECuCl$_2$]** with a propylene linker unit between the imine and amine moieties, exhibited the highest catalytic activity (1.95×10^4 g PMMA per mol Cu h), yielding the high-molecular-weight PMMA. All the complexes furnished syndiotactic PMMA regardless of the ligand architecture. Dimethyl Cu(II) complexes **[L_nCuMe$_2$]** (L_n = L_A–L_F), generated *in situ*, demonstrated high activities towards *rac*-LA and yielded highly hetero-enriched PLA. Varying the substituents of the imine moiety influenced the polymerization of *rac*-LA: the steric (and electronic) properties of the substituents appended to the iminopyridine greatly affected their catalytic activity and stereoselectivity. All the resultant PLAs displayed high molecular weights and slightly broader PDIs. Microstructural analysis of the PLAs generated showed enhanced heterotactic enchainment at lower temperatures compared to that at room temperature.

Conflicts of interest

There are no conflicts to declare.

Acknowledgements

This research was supported by the National Research Foundation (NRF) of South Korea, funded by the Ministry of the Education, Science, and Technology (MEST) (Grant No. 2019R1A2C1088654). X-ray crystallography with PLS-II 2D-SMC beamline was supported by MSIP and POSTECH.

References

1 Z. Cimerman, S. Miljanić and N. Galić, Schiff Bases Derived from aminopyridines as spectrofluorimetric analytical reagents, *Croat. Chem. Acta*, 2000, **73**, 81–95.
2 R. Miri, N. Razzaghi-asl and M. K. Mohammadi, QM study and conformational analysis of an isatin Schiff base as a potential cytotoxic agent, *J. Mol. Model.*, 2013, **19**, 727–735.
3 W. A. Zoubi, Biological activities of Schiff bases and their complexes: a review of recent works, *Int. J. Org. Chem.*, 2013, **3**, 73–95.
4 K. Brodowska and E. Łodyga-Chruścińska, Schiff bases–interesting range of applications in various fields of science, *Chemik*, 2014, **68**, 129–134.
5 A. D. Garnovskii and I. S. Vasil'Chenko, Rational design of metal coordination compounds with azomethine ligands, *Russ. Chem. Rev.*, 2002, **71**, 943–968.
6 T. S. B. Baul, S. Kundu, S. W. Ng, N. Guchhait and E. R. T. Tiekink, Synthesis, characterization, photoluminescent properties and supramolecular aggregations in diimine chelated cadmium dihalides, *J. Coord. Chem.*, 2014, **67**, 96–119.
7 M. Shyamal, A. Panja and A. Saha, Five new mononuclear zinc(II) complexes with a tetradentate N-donor Schiff base: syntheses, structures and influence of anionic coligands on the luminescence behaviour and supramolecular interactions, *Polyhedron*, 2014, **69**, 141–148.
8 K. C. Gupta and A. K. Sutar, Catalytic activities of Schiff base transition metal complexes, *Coord. Chem. Rev.*, 2008, **252**, 1420–1450.
9 P. G. Cozzi, Metal-Salen Schiff base complexes in catalysis: practical, *Chem. Soc. Rev.*, 2004, **33**, 410–421.
10 B. Türkkan, B. Sarıboğa and N. Sarıboğa, Synthesis, characterization and antimicrobial activity of 3,5-di-*tert*-butylsalicylaldehyde-*S*-methylthiosemicarbazones and their Ni(II) complexes, *Transition Met. Chem.*, 2011, **36**, 679–684.
11 V. L. Siji, M. R. Sudarsanakumar and S. Suma, Synthesis, spectroscopic characterization, and antimicrobial activity of cobalt(II) complexes of acetone-*N*(4)-phenylsemicarbazone: crystal structure of $[Co(HL)_2(MeOH)_2](NO_3)_2$, *Transition Met. Chem.*, 2011, **36**, 417–424.
12 C. V. K. Sharma, Crystal engineering-where do we go from here?, *Cryst. Growth Des.*, 2002, **2**, 465–474.
13 I. Ahamad, R. Prasad and M. A. Quraishi, Thermodynamic, electrochemical and quantum chemical investigation of some Schiff bases as corrosion inhibitors for mild steel in hydrochloric acid solutions, *Corros. Sci.*, 2010, **52**, 933–942.
14 N. K. Al Rasbi and J. Husband, Excitation and emission properties of Zn(II) Schiff base complex by combined crystallographic, spectroscopic and DFT studies, *J. Photochem. Photobiol., A*, 2016, **314**, 96–103.
15 N. Raman, A. Kulandaisamy, C. Thangaraja and K. Jeyasubramanian, Redox and antimicrobial studies of transition metal(II) tetradentate Schiff base complexes, *Transition Met. Chem.*, 2003, **28**, 29–36.
16 G. G. Mohamed, Synthesis, characterization and biological activity of bis(phenylimine) Schiff base ligands and their metal complexes, *Spectrochim. Acta, Part A*, 2006, **64**, 188–195.
17 Z. Liu, J. Zhang, T. Li, Z. Yu and S. Zhang, Fourinated hydrogen bonding liquid crystals based on Schiff base, *J. Fluorine Chem.*, 2013, **147**, 36–39.
18 H. Kotzé and S. Mapolie, Cationic ruthenium(II) complexes supported on mesoporous silica as catalyst precursors in the selective oxidative cleavage of 1-octene, *Appl. Organomet. Chem.*, 2017, **31**, 1–13.
19 M. H. Soliman, G. G. Mohamed and E. A. Mohamed, Metal complexes of fenoterol drug: preparation, spectroscopic, thermal, and biological activity, *J. Therm. Anal. Calorim.*, 2010, **99**, 639–647.

20 C. Bianchini, G. Mantovani, A. Meli, F. Migliacci and F. Laschi, Selective oligomerization of ethylene to linear α-olefins by tetrahedral cobalt(II) complexes with 6-(organyl)-2-(imino)pyridyl ligands: influence of the heteroatom in the organyl group on the catalytic activity, *Organometallics*, 2003, **22**, 2545–2547.

21 Q. Mahmood, J. Guo, W. Zhang, Y. Ma, T. Liang and W.-H. Sun, Concurrently improving the thermal stability and activity of ferrous pre-catalysts for the production of saturated/unsaturated polyethylene, *Organometallics*, 2018, **37**, 957–970.

22 C.-Y. Hsiao, H.-A. Han, G.-H. Lee and C.-H. Peng, AGET and SARA ATRP of styrene and methyl methacrylate mediated by pyridyl-imine based copper complexes, *Eur. Polym. J.*, 2014, **51**, 12–20.

23 I. Kim, J. -M. Hwang, J. K. Lee, C. S. Ha and S. I. Woo, Polymerization of methyl methacrylate with Ni(II) α-diimine/MAO and Fe(II) and Co(II) pyridyl bis(imine)/MAO, *Macromol. Rapid Commun.*, 2003, **24**, 508–511.

24 A. Menteş and M. E. Hanhan, Synthesis of water-soluble Mo(0) tetracarbonyl complexes containing nitrogen donor ligands and polymerization of methyl methacrylate, *Transition Met. Chem.*, 2008, **33**, 91–97.

25 J. C. Worch, H. Prydderch, S. Jimaja, P. Bexis, M. L. Becker and A. P. Dove, Stereochemical enhancement of polymer properties, *Nat. Rev. Chem.*, 2019, **3**, 514–535.

26 M. A. Giardello, Y. Yamamoto, L. Brard and T. J. Marks, Stereocontrol in the polymerization of methyl methacrylate mediated by chiral organolanthanide metallocenes, *J. Am. Chem. Soc.*, 1995, **117**, 3276–3277.

27 H. Yasuda, H. Yamamoto, M. Yamashita, K. Yokota, A. Nakamura, S. Miyake, Y. Kai and N. Kanehisa, Synthesis of high molecular weight poly(methyl methacrylate) with extremely low polydispersity by the unique function of organolanthanide(III) complexes, *Macromolecules*, 1993, **26**, 7134–7143.

28 I. Kim, J.-M. Hwang, J. K. Lee, C. S. Ha and S. I. Woo, Polymerization of methyl methacrylate with Ni(II) α-diimine/MAO and Fe(II) and Co(II) pyridyl bis(imine)/MAO, *Macromol. Rapid Commun.*, 2003, **24**, 508–511.

29 L. Yao, L. Wang, J. Zhang, N. Tang and J. Wu, Ring opening polymerization of L-lactide by an electron-rich Schiff base zinc complex: an activity and kinetic study, *J. Mol. Catal. A: Chem.*, 2012, **352**, 57–62.

30 K. S. Kwon, S. Nayab and J. H. Jeong, Synthesis, characterisation and X-ray structures of zinc(II) complexes bearing camphor-based iminopyridines as pre-catalysts for heterotactic-enriched polylactide from *rac*-lactide, *Polyhedron*, 2015, **85**, 615–620.

31 X. W. Zhang and G.-X. Jin, Polymerized metallocene catalyst and late transition metal catalysts for ethylene polymerization, *Coord. Chem. Rev.*, 2006, **250**, 95–109.

32 V. C. Gibson, R. K. O'Reilly, D. F. Wass, A. J. P. White and D. J. Williams, Iron complexes bearing iminopyridine and aminopyridine ligands as catalysts for atom transfer radical polymerisation, *Dalton Trans.*, 2003, 2824–2830.

33 J. Heo, H. Lee and S. Nayab, Polymerizations of methyl methacrylate and *rac*-lactide by zinc(II) precatalyst containing *N*-substituted 2-iminomethylpyridine and 2-iminomethylquinoline, *J. Coord. Chem.*, 2017, **70**, 3837–3858.

34 Y. Song, D. Kim, H.-J. Lee and H. Lee, Cd(II) and Zn(II) complexes containing *N*,*N*′-bidentate *N*-(pyridin-2-ylmethylene)cyclopentanamine: synthesis, characterisation and methyl methacrylate polymerisation, *Bull. Korean Chem. Soc.*, 2014, **35**, 2929–2934.

35 S. Kim, E. Kim, H.-J. Lee and H. Lee, Palladium(II) complexes containing *N*,*N*′-bidentate *N*-cycloalkyl 2-iminomethylpyridine and 2-iminomethylquinoline: synthesis, characterisation and methyl methacrylate polymerisation, *Polyhedron*, 2014, **69**, 149–155.

36 D. Kim, Y. Song, S. Kim, H.-J. Lee and H. Lee, *N*,*N*′,*X*-bidentate *versus* *N*,*N*′,*X*-tridentate *N*-substituted 2-iminomethylpyridine and 2-iminomethylquinoline-coordinated palladium(II) complexes, *J. Coord. Chem.*, 2014, **67**, 2312–2329.

37 S. Park, J. Lee, H. Lee, A. R. Jeong, K. S. Min and S. Nayab, Five-coordinate dinuclar cobalt(II), copper(II), zinc(II) and cadmium(II) complexes with 4-bromo-*N*-(2-pyridinylmethylene)benzenamine: synthesis, characterisation and methyl methacrylate polymerization, *Appl. Organomet. Chem.*, 2019, **33**, 1–11.

38 J. Lee, H. Lee, S. Nayab and K. B. Yoon, Synthesis, characterization and polymerisation studies of cadmium(II) complexes containing *N*,*N*′,*X*-tridentate *X*-substituted (X = N, O) 2-iminomethylpyridines, *Polyhedron*, 2019, **158**, 432–440.

39 G. Zakrzewski and L. Sacconi, Four-, five-, and six-coordinated nickel(II) and cobalt(II) complexes of Schiff bases derived from pyridine-2-carboxaldehyde and *N*,*N*-substituted ethylenediamines, *Inorg. Chem.*, 1968, **7**, 1034–1036.

40 B. de Klerk-Engels, H.-W. Frühauf, K. Vrieze, H. Kooijman and A. L. Spek, Kinetic and thermodynamic products in the reaction of $[RuCl_2(CO)_2]_n$ with pyridinecarbaldimine ligands and the crystal structure of trans-$Cl_2Ru(CO)_2$(*N*-(pyrid-2-ylmethoxymethyl)(3-isopropoxypropyl)amine), *Inorg. Chem.*, 1993, **32**, 5528–5535.

41 T. K. Maji, P. S. Mukherjee, G. Mostafa, T. Mallah, J. Cano-Boquera and N. R. Chaudhuri, First observation of a ferromagnetic interaction through an end-to-end azido bridging pathway in a 1D copper(II) system, *Chem. Commun.*, 2001, 1012–1013.

42 W.-B. Yuan and Q. Zhang, Dichloro[*N*,*N*-dimethyl-*N*′-(2-pyridylmethylidene)ethane-1,2-diamine]copper(II), *Acta Crystallogr., Sect. E: Struct. Rep. Online*, 2005, **61**, 1883–1884.

43 A. Bhattacharjee, S. Halder, K. Ghosh, C. Rizzoli and P. Roy, Mono-, tri- and polynuclear copper(II) complexes of Schiff-base ligands: synthesis, characterization and catalytic activity towards alcohol oxidation, *New J. Chem.*, 2017, **41**, 5696–5706.

44 T. J. J. Whitehorne and F. Schaper, Square-Planar Cu(II) diketiminate complexes in lactide polymerization, *Inorg. Chem.*, 2013, **52**, 13612–13622.

45 B. M. Chamberlain, M. Cheng, D. R. Moore, T. M. Ovitt, E. B. Lobkovsky and G. W. Coates, Polymerization of lactide with zinc and magnesium α-diiminate complexes: stereocontrol and mechanism, *J. Am. Chem. Soc.*, 2001, **123**, 3229–3238.

46 T. Zell, B. E. Padden, A. J. Paterick, K. A. M. Thakur, R. T. Kean, M. A. Hillmyer and E. J. Munson, Unambiguous determination of the ^{13}C and ^{1}H NMR stereosequence assignments of polylactide using high-resolution solution NMR spectroscopy, *Macromolecules*, 2002, **35**, 7700–7707.

47 Y. Isobe, T. Nakano and Y. Okamoto, Stereocontrol during the free-radical polymerization of methacrylates with Lewis acids, *J. Polym. Sci., Part A: Polym. Chem.*, 2001, **39**, 1463–1471.

48 T. Kitaura and T. Kitayama, Anionic polymerization of methyl methacrylate with the aid of lithium trimethylsilanolate (Me_3SiOLi) –superior control of isotacticity and molecular weight, *Macromol. Rapid Commun.*, 2007, **28**, 1889–1893.

49 A. J. Arvai and C. Nielsen. *ADSC Quantum-210 ADX Program*, Area Detector System Corporation, Poway, CA, USA, 1983.

50 Z. Otwinowski and W. Minor, [20] Processing of X-ray diffraction data collected in oscillation mode, *Methods in Enzymology*, ed. C. W. Carter Jr and R. M. Sweet, Academic Press, New York, 1997, part A, vol. 276, pp. 307–324.

51 G. M. Sheldrick, A short history of SHELX, *Acta Crystallogr., Sect. A: Found. Crystallogr.*, 2008, **64**, 112–122.

52 Z. Zhong, P. J. Dijkstra and J. Feijen, Controlled and stereoselective polymerization of lactide: kinetics, selectivity, and microstructures, *J. Am. Chem. Soc.*, 2003, **125**, 11291–11298.

53 Z. Kan, W. Luo, T. Shi, C. Wei, B. Han, D. Zheng and S. Liu, Facile preparation of stereoblock PLA From ring-opening polymerization of *rac*-lactide by a synergetic binary catalytic system containing ureas and alkoxides, *Front. Chem.*, 2018, **6**, 547–555.

54 E. Castro, M. J. Percino, V. M. Chapela, M. Ceron, G. Soriano-Moro, J. Lopez-Cruz and F. J. Melendez, Theoretical and experimental spectroscopic analysis of cyano-substituted styrylpyridine compounds, *Int. J. Mol. Sci.*, 2013, **14**, 4005–4029.

55 M. Hosny, Synthesis and characterization of transition metal complexes derived from (*E*)-*N*-(1-(pyridine-2yl)ethylidiene) benzohydrazide (PEBH), *Synth. React. Inorg., Met.-Org., Nano-Met. Chem.*, 2011, **41**, 736–742.

56 Y. Song, D. Kim, H.-J. Lee and H. Lee, Synthesis and structural characterization of $[(dpca)MX_2]$ (M = Cu, X = Cl; M = Cd, X = Brand, M = Zn, X = NO_3) complexes containing *N*,*N*-di(2-picolyl)cyclohexylamine (dpca) and their application to methyl methacrylate polymerization, *Inorg. Chem. Commun.*, 2014, **45**, 66–70.

57 S. Salga, H. Khaledi, H. M. Ali and R. Puteh, Dichlorido{*N*,*N*-dimethyl-*N*′-[1-(2pyridyl)ethylidene]ethane-1,2-diamineκ^3N,N',N''}copper(II), *Acta Crystallogr., Sect. E: Struct. Rep. Online*, 2010, **66**, m508.

58 S. A. Turner, Z. D. Remillard, D. T. Gijima, E. Gao, R. D. Pike and C. Goh, Syntheses and structures of closely related copper(I) complexes of tridentate (2-pyridylmethyl)imine and (2-pyridylmethyl)amine ligands and their use in mediating atom transfer radical polymerizations, *Inorg. Chem.*, 2012, **51**, 10762–10773.

59 Y.-X. Sun, Synthesis, Crystal Structures and Antibacterial Activities of Two Schiff Base Copper(II) Complexes, *Synth. React. Inorg., Met.-Org., Nano-Met. Chem.*, 2006, **36**, 621–625.

60 A. W. Addison, T. N. Rao, J. Reedijk, J. van Rijn and G. C. Verschoor, Synthesis, Structure, and spectroscopic properties of copper(II) compounds containing nitrogen-sulphur donor ligands; the crystal and molecular structure of aqua[l,7-bis(*N*-methylbenzimidazol-2'-yl)-2,6-dithiaheptane]copper(II)perchlorate, *J. Chem. Soc., Dalton Trans.*, 1984, 1349–1356.

61 D. C. Crans, M. L. Tarlton and C. C. Mclauchlan, Trigonal bipyramidal or square pyramidal coordination geometry? Investigating the most potent geometry for vanadium phosphatase inhibitors, *Eur. J. Inorg. Chem.*, 2014, 4450–4468.

62 L. Yang, D. R. Powell and R. P. Houser, Structural variation in copper(I) complexes with pyridylmethylamide ligands: structural analysis with a new four-coordinate geometry index, τ_4, *Dalton Trans.*, 2007, 955–964.

63 D. J. Darensbourg, Making plastics from carbon dioxide: salen metal complexes as catalysts for the production of polycarbonates from epoxides and CO_2, *Chem. Rev.*, 2007, **107**, 2388–2410.

64 G.-P. Wu, D. J. Darensbourg and X.-B. Lu, Tandem metal-coordination copolymerization and organocatalytic ring-opening polymerization *via* water to synthesize diblock copolymers of styrene oxide/CO_2 and lactide, *J. Am. Chem. Soc.*, 2012, **134**, 17739–17745.

65 S. Shin, S. Nayab and H. Lee, Polymerizations of methyl methacrylate and *rac*-lactide by 4-coordinate cobalt(II) complexes supported by *N*′-substituted *N*,*N*′,*N*-bis((1*H*-pyrazol-1-yl)methyl)amine derivatives, *Polyhedron*, 2018, **141**, 309–321.

66 S. Shin, H. Cho, H. Lee, S. Nayab and Y. Kim, Zinc(II) complexes containing *N*′-aromatic group substituted *N*,*N*′,*N*-bis((1*H*-pyrazol-1yl)methyl)amines: synthesis, characterization, and polymerizations of methyl methacrylate and *rac*-lactide, *J. Coord. Chem.*, 2018, **71**, 556–584.

67 J.-C. Wu, B.-H. Huang, M.-L. Hsueh, S.-L. Lai and C.-C. Lin, Ring-opening polymerization of lactide initiated by magnesium and zinc alkoxides, *Polymer*, 2005, **46**, 9784–9792.

68 M. A. Masuelli, Mark-Houwink parameters for aqueous-soluble polymers and biopolymers at various temperatures, *J. Polym. Biopolym. Phys. Chem.*, 2014, **2**, 37–43.

69 H. R. Kricheldorf, S.-R. Lee and S. Bush, Polylactones 36. Macrocyclic polymerization of lactides with cyclic Bu_2Sn initiators derived from 1,2-ethanediol, 2-mercaptoethanol,

and 1,2-dimercaptoethane, *Macromolecules*, 1996, **29**, 1375–1381.

70 N. Ajellal, D. M. Lyubov, M. A. Sinenkov, G. K. Fukin, A. V. Cherkasov, C. M. Thomas, J.-F. Carpentier and A. A. Trifonov, Bis(guanidinate) alkoxide complexes of lanthanides: synthesis, structures and use in immortal and stereoselective ring-opening polymerization of cyclic esters, *Chem.–Eur. J.*, 2008, **14**, 5440–5448.

71 D. J. Darensbourg and O. Karroonnirun, Ring-opening polymerization of lactides catalyzed by natural amino-acid based zinc catalysts, *Inorg. Chem.*, 2010, **49**, 2360–2371.

72 H. Cho, M. J. Jung, J. Jeon, H. Lee and S. Nayab, Synthesis, structural characterization and MMA polymerization studies of dimeric 5-coordinate copper(II), cadmium(II), and monomeric 4-coordinate zinc(II) complexes supported by *N*-methyl-*N*-((pyridine-2-yl)methyl) benzeneamine, *Inorg. Chim. Acta*, 2019, **487**, 221–227.

73 Y. Song, D. Kim, H.-J. Lee and H. Lee, Synthesis and structural characterization of [(dpca)MX_2] (M = Cu, X = Cl; M = Cd, X = Br and M = Zn, X = NO_3) complexes containing *N*,*N*-di(2-picolyl)cyclohexylamine (dpca) and their application to methyl methacrylate polymerization, *Inorg. Chem. Commun.*, 2014, **45**, 66–70.

74 C. Lansalot-Matras, F. Bonnette, E. Mignard and O. Lavastre, *N*-tripodal ligands to generate copper catalysts for the syndiotactic polymerization of methyl-methacrylate: crystal structures of copper complexes, *J. Organomet. Chem.*, 2008, **693**, 393–398.

75 L.-L. Miao, H.-X. Li, M. Yu, W. Zhao, W.-J. Gong, J. Gao, Z.-G. Ren, H.-F. Wang and J.-P. Lang, Preparation of a nitrate-coordinated copper(II) complex of 2-(pyrazol-3-yl)-6-(pyrazolate)pyridine as an efficient catalyst for methyl methacrylate polymerization, *Dalton Trans.*, 2012, **41**, 3424–3430.

